Nov 11th, 12:00 AM

Column Behaviour of Cold-formed Hollow Sections

Peter W. Key

S. W. Hasan

Gregory J. Hancock

Eighth International Specialty Conference on Cold-Formed Steel Structures
St. Louis, Missouri, U.S.A., November 11-12, 1986

COLUMN BEHAVIOUR OF COLD-FORMED HOLLOW SECTIONS

P. W. KEY *, S. W. HASAN* AND G. J. HANCOCK**

Summary

The results of an experimental investigation into the strength and collapse behaviour of Australian produced cold-formed square and rectangular hollow section columns is described. The individual plate strengths calculated from the stub column tests on both square and rectangular hollow sections are compared with predictions based on the effective width formulae in the AISI Specification. The long column test results on square hollow sections are compared with the AISI Class A and Class B column curves as well as a proposal based on the SSRC multiple column curves.

The sections studied had plate width to thickness ratios in a range where local buckling and yielding occur almost simultaneously, leading to rapid load shedding after ultimate. Theoretical models of the post-ultimate collapse behaviour, based on local plastic mechanisms, are summarised in the paper. The theoretical models are compared with the collapse behaviour of the stub columns and long columns.

* Postgraduate Student, School of Civil and Mining Engineering, University of Sydney, N.S.W., Australia, 2006.

** Associate Professor, School of Civil and Mining Engineering, University of Sydney

1. Introduction

The use of square and rectangular hollow sections manufactured by cold-forming has increased worldwide as research into their strength and applicability has continued (Refs. 3,8,9,17). Sections of this type, which have not been stress relieved by hot finishing processes, usually have an enhanced yield strength in both their corners and flats as a result of the cold-forming operations. However, a reduced material ductility can occur as a result of the strain-hardening of the steel during the manufacturing operation. In addition, if the sections are formed from thin strip so that the local buckling load and yield load of the section in pure compression are approximately equal, then a rapid drop in load capacity may occur after the maximum load has been reached. Tests of cold-formed rectangular and square hollow sections with moderately slender faces (b/t in range approximately 30 to 50) are described in this paper.

Two test series were performed. The first consisted of stub columns tested between rigid frictionless platens. The tests were performed on both rectangular and square hollow sections with a view to determining the limiting plate slenderness beyond which the plate was not fully effective in compression. These test results are compared with the relevant formulae in the AISI Specification (Ref. 1). The second series consisted of long columns tested between spherical end bearings to determine their load capacity for comparison with existing and proposed (Ref. 7) column curves. This latter series was performed on square hollow section columns. The test results are compared with the AISI Class A and Class B column curves (Ref. 17) and a proposal for the Australian Limit State Steel Structures Code which uses column curves developed by Rotter (Ref. 16) which are based on the SSRC Multiple Column Curves (Ref. 7).

The columns tested were all controlled using axial shortening measured using an extensometer located between the end bearings of the test rig. Consequently, the unloading of the specimens after ultimate could be followed provided that the axial shortening did not decrease after ultimate. Hence the post-ultimate load-shortening characteristics of the sections were determined. Sections with slender faces usually develop inelastic local buckles which lead to a rapid drop in load capacity. Models of these inelastic local buckles, called spatial plastic mechanisms, have been proposed previously for channel sections and stiffened plates (Ref. 14), and for box columns with angular corners (Refs. 12,15). In this paper, spatial plastic mechanisms proposed for square and rectangular hollow sections with rounded corners are compared with the post-ultimate behaviour determined by testing. Two different spatial plastic mechanisms are proposed. The first is for stub columns where all four faces at a cross section deform simultaneously. The second is for pin-ended columns where the spatial plastic mechanism, which is usually in the centre of the column, involves local buckling of only three faces as a result of the combined bending and compression.

2. Scope of Investigation

Four different cross section sizes of square shape (SHS) and six different sizes of rectangular shape (RHS) were chosen for testing from the manufacturer's catalogue of hollow sections. Sections with higher plate slenderness were chosen in order to investigate the effect of inelastic local buckling on the column strength and post-ultimate response. The stub column sizes tested are given in Table II and the pin-ended column sizes tested are

given in Table III where the specimen dimensional notation is given in Fig. 1(a). All test material was strain aged at 150 degrees Centigrade for 15 minutes prior to testing. Test specimens for any one section size were supplied from the same rolling except for the 76.0 mm (3.0 in) square hollow section for which two test series (numbered 1 and 2) were performed.

Electrical resistance strain gauges, attached to the surface of the section as shown in Fig. 1(b), were used to determine the residual stresses by measuring the change in strain as the section was cut into longitudinal strips. The magnitude and distribution of material properties around the sections were measured using tensile coupons. Typically, three coupons were taken from each face (one on the centreline and the other two as close to each corner as practicable) and one from each corner of each section size. Initial column out-of-straightness was measured using a precision optical level with micrometer and microstaff placed at a sufficient number of points along the horizontally supported member to clearly define the shape and maximum out-of-straightness.

The stub column preparation and testing were performed in accordance with the recommendations set out in Ref. 7. Pin-ended column tests were carried out in a specially constructed horizontal column testing rig based on a DARTEC 2000 kN capacity servo-controlled hydraulic loading ram located in a reaction frame which could support specimens up to 10 m (32.8 ft) long. Tests were performed under extensometer control which allowed the unloading curve to be followed provided that the extension increased monotonically. Spherical pinned bearings at each end of the specimen under test allowed end rotation about perpendicular axes. The pin-ended columns were tested at four different overall slenderness values (see Table III) and at eccentricities of zero (concentric) and approximately L/1000 (eccentric). Further details are given in Ref. 10.

3. Residual Stresses

The longitudinal residual stresses, which were computed from the measured residual strains by simply multiplying by the Young's modulus, were found to be generally tensile on the outer surface and compressive on the inner surface. The resulting membrane component is shown in Fig. 2(a) and through thickness bending component is shown in Fig. 2(b). The membrane residual stress does not exceed approximately 15 percent of the actual yield stress, while the through thickness residual stresses are up to 70 percent of the yield stresses. These values are in agreement with other studies (Ref. 4) which have shown the through thickness component of residual stress to be an important factor affecting the column maximum strength.

4. Material Properties

Tensile coupons taken from the faces of the sections generally displayed a distinct though limited yield plateau in their stress-strain behaviour (Fig. 3(a)), while the corner regions displayed gradual yielding typical of highly worked material (Fig. 3(b)). The yield stress or 0.2 percent proof stress (σ_y) and ultimate tensile strength (σ_u), based on average face and corner values, are given for all sections in Table I. A typical distribution of yield stress and ultimate tensile strength around a section is given in Fig. 3(c).

The values of uniform elongation , taken to the ultimate stress and not fracture, are also given for the corner and face specimens in Table II. Ductility has been reduced from that of the unformed material which was measured to have a uniform elongation at ultimate in the range 15 to 20 percent. Dhalla and Winter (Ref. 5) recommend that for ductile behaviour, the material should have a uniform elongation greater than 3 percent and an ultimate to yield ratio of 1.05 . In general, the cold-worked sections have a uniform elongation on the faces in the range 5.4 to 9.6 percent and a uniform elongation in the corners in the range 2.3 to 4.3 percent, except for the 203 mm (8 in) by 102 mm (4 in) by 4.9 mm (0.20 in) thick rectangular section.

5. Stub Column Tests

5.1 Test Results

The maximum loads obtained from the stub column tests (P_{Sult}) are presented in Table II, together with the computed tensile coupon yield load (P_{Scoup}) which is an area weighted function of the average face and average corner yield stresses for each section based on the full section area. The fact that the ratio of P_{Sult}/P_{Scoup} is less than unity for the sections with higher plate slenderness values indicates that inelastic local buckling has influenced the maximum load.

Typical load-extension plots for two sections are shown in Figs. 4(a) and 4(b). For the section in Fig. 4(a), which had a face slenderness (w/t) of 33.0, rapid load shedding occurred immediately after ultimate as a result of the formation of spatial plastic mechanisms in the four faces of the section. For the section in Fig. 4(b), which had a face slenderness (w/t) of 26.0, a short yield plateau occurred before formation of the spatial plastic mechanism and the associated rapid load shedding.

5.2 Strength Formulae

Theoretical calculation of the stub column strength depends upon the values and distribution of yield stress assumed as well as the effective width formula used to calculate the effective portions of slender faces. For the purpose of calculating the limiting plate slenderness beyond which the flat face of a cold formed rectangular or square hollow section is no longer fully effective, the load carried by the flat face (P_{slf}), non-dimensionalised with respect to its squash load (P_y), has been plotted against the non-dimensionalised plate slenderness (S) in Fig. 5. The load carried by a single flat face of a square hollow section has been determined by subtracting the load carried by the corners, based on the actual corner yield stress, from the stub column strength and dividing by 4. In the case of the rectangular hollow sections, the stockier faces have been assumed to carry their squash load and so the load carried by the stocky faces has also been subtracted and the resulting load divided by 2. The non-dimensionalised plate slenderness defined by Equation 1 has been used to allow for the different values of yield strength in the faces of the different sections.

$$S = (w/t)\sqrt{\{12\sigma_y(1-\nu^2)/\pi^2 EK\}} \qquad (1)$$

The curves representing local buckling, Von Karman plate strength and the AISI effective width formula for closed square and rectangular tubes have also been plotted in Fig. 5. The local buckling coefficient, K , has been taken as

4.0 in all calculations. Although the local buckling coefficient may be greater than 4.0 for the slender faces, when the restraint provided by the stocky faces is included, tests by Moxham (Ref. 13) on simply supported and restrained plates indicate that there is very little increase in strength for plates with restrained longitudinal edges. Hence the use of a value of 4.0 in strength calculations seems justified.

The cut-off value of S at which the plate is no longer fully effective is approximately 0.73. For a plate with a yield strength of 250 MPa (36.3 ksi), the w/t value is 39.3 and for a plate with a yield strength of 350 MPa (50.8 ksi), the w/t value is 33.3. Insufficient tests were available to check the validity of the effective width formula at high slenderness values. However, the point at which the effective width is not equal to the full width appears to be accurately predicted by the AISI limit.

6. Long Column Tests

6.1 Geometric Imperfections

Out-of straightness measurements taken on the longer 76 mm (3.0 in), 152 mm (6.0 in) and 203 mm (8.0 in) square sections typically revealed a single curvature profile with an average out-of-straightness of L/6600 and L/11000 about each axis respectively. A minimum value of L/5100 was recorded. Detailed profiles are given in Ref. 10.

6.2 Test Results

The pin-ended column test results are summarised in Table III. Typical column load-axial deformation curves are shown for a 76 mm (3.0 in) square section in Fig. 6 at two different overall column slenderness ratios. The rapid load shedding following inelastic local buckling is clearly evident in both these curves.

6.3 Column Design Curves

6.3.1 AISI Column Design Curves

The American Iron and Steel Institute (AISI) column curves were developed by Sherman (Ref. 17) based on available test data for both hot formed and cold formed rectangular hollow sections. Two curves were proposed: Class A for tubular hollow sections (hot or cold formed) and hot formed or cold formed stress relieved rectangular sections; Class B for cold formed rectangular hollow sections. The Class A column curve is the same as that already used in the AISI Specification (Ref. 1). To take account of local buckling, Sherman has used the same Q factor as already defined in the AISI Specification.

The theoretically computed values of $Q_f P_{yf}$, based on the mean face yield strength of each specimen given in Table I, are set out in Table II. They are slightly lower than the measured stub column strengths probably as a result of the enhanced yield strengths in the corners of the tubular sections. The pin-ended column test results on the square hollow sections are compared in Fig. 7 with the unfactored AISI Class A and Class B column curves. The loads have been nondimensionalised with respect to the stub column strength ($Q_f P_{yf}$) and plotted against the nondimensionalised slenderness to allow a comparison of all test results on the one graph. The unfactored Class A column curve provides a reasonable estimate of the concentrically loaded column tests. The unfactored Class B column curve is very conservative at low slenderness values and approximates the eccentrically loaded tests at high slenderness values.

6.3.2 Australian Limit State Steel Structures Code Column Curves

The Australian Steel Structures Code (Ref. 2) is currently being revised in limit state format. As part of this revision, the concept of multiple column curves, as typified by the SSRC Column Curves (Ref. 7), is being introduced to allow for different column strength characteristics of different column types. A proposal for determining multiple column curves based on the use of modified slenderness was proposed by Rotter (Ref. 16).

The test results on the long columns are compared with three such curves in Fig. 8. The test strengths have been non-dimensionalised with respect to the stub column strength ($Q_f P_{yf}$) based on the mean face yield strength given in Table I. The values of Q_f are based on the limiting slenderness beyond which a plate element of a cold formed tube is not fully effective as defined in the Australian Steel Structures Code (Ref. 2). The limiting slenderness defined in Ref. 2 is $635/\sqrt{(\sigma_y}$ in MPa) ($242/\sqrt{(\sigma_y}$ in ksi) based on the clear widths b,d defined in Fig. 1(a). The resulting stub column strengths are given in the final column of Table II.

The upper and lower curves in Fig. 8 with c equal to -1.0 and 0.0 correspond approximately with the SSRC1 and SSRC2 column curves respectively. The test results on the eccentrically loaded columns are approximated by the curve with c equal to -0.5 and this has been proposed for the new Australian standard.

7 Post-Ultimate Behaviour

7.1 Stub Column Spatial Plastic Mechanisms

A typical stub column after development of the spatial plastic mechanism is shown in Fig. 9. Each face of the section behaves essentially in a similar manner, two opposite faces folding inwards, the remaining two folding outwards. The corners of the section are of a finite radius and do not appear to participate in the spatial plastic mechanism as they would if they were angular and failed in the mechanism described in Ref. 15. Consequently, the resulting mechanism will be a pseudo-mechanism (Ref. 14) where a degree of in-plane movement resulting from yielding of the corners occurs.

The assumed theoretical model used for the analysis of stub column behaviour is shown in Fig. 10(a). The model is analysed as three basic components, being:

(a) Plate folding mechanism
(b) Corner yielding
(c) Folding corner restraint.

Each of these components is described briefly below. The detailed derivation and descriptions are given in Ref. 11.

The plate folding mechanism for each face consists of three plastic hinges along lines ab, cd and ef as shown in Fig. 10(a). The hinges are modelled as straight although in reality they are slightly curved as shown in Fig. 9. The compressive force in one face (P_A) can be related to the out-of-plane displacement of the mechanism (Δ) as given by Equation 2.

$$P_A = \sigma_{yf}\, t\, b_2[\sqrt{\{(\Delta/t)^2 + 1\}} - \Delta/t] \quad (2)$$

where σ_{yf} is the face yield stress.

To retain a kinematically admissible mechanism, the corner regions must undergo axial deformation equal to that due to the plate folding mechanism. Under even moderately small folding deformation, the axial strain, induced in the corners is above the yield strain. Hence it is assumed that the full corner areas are at yield equal to that of the corners as given in Table I. The resulting equation for P_B , the axial force in the corners is given by Equation 3.

$$P_B = \sigma_{yc}\, A_c \quad (3)$$

where σ_{yc} is the corner yield stress and A_c is the corner area.

The opening of the corner regions of the plate folding mechanism shown in Fig. 10(a) is obviously kinematically inadmissible. Experimental observations indicate that to retain compatibility between the folding plates and corners, the longitudinal edges of each plate mechanism are bent plastically as deformations grow as shown in Fig. 11(b). The restraining force F_R applied to each side of the plate folding mechanism can be calculated by applying equilibrium to the corner element in Fig. 11(c). The effect on the restraining force F_r of torsional restraint to twisting of the corner element has been calculated based on the plastic torsional rigidity (Ref. 6) and found to be small. The resulting additional load component in the plates (P_C) can be calculated using the principle of virtual work and is given by Equation 4.

$$P_C = \sigma_{yc}\, t\, \alpha^2\, b_2^2/16\Delta\beta \quad (4)$$

where βt is the centreline corner radius and αb_2 is the mechanism length.

The total load (P_{smech}) is the sum of the three components (P_A, P_B, P_C) taken over the four faces and corners. The total axial deformation is the sum of the axial deformation due to geometric changes in the spatial plastic mechanism and the elastic deformation due to the applied load. The total axial deformation (e_{tot}) is given by Equation 5.

$$e_{tot} = 2\Delta^2/\alpha b_2 + P_{smech}\, L/EA \quad (5)$$

where L is the stub column length and A is the total section area.

The total load and its three components are shown for the 76mm (3.0 in) and 152 mm (6.0 in) sections in Figs. 4(a) and 4(b) respectively. In both cases the agreement between the experiment and the model is good except that the length of the plastic plateau of the 152 mm section is not fully realised in the model. The magnitude of the folding restraint component (P_C) decreases markedly as the deformations increase.

7.2 Pin-ended Column Spatial Plastic Mechanism

The majority of hollow sections used in practice are not constrained to buckle simultaneously on all faces since the column ends have a degree of rotational freedom to allow asymmetrical local buckling. Consequently the spatial plastic mechanism is asymmetric of the type shown in Fig. 10(b). In this case, plate folding mechanisms occur in only three faces of the column with a hinge line (ef) occuring on the fourth face. The detailed analysis of this mechanism is given in Ref. 11. It is considerably more complex analytically than the stub column mechanism since the line of action of the total load will vary as the mechanism translates sideways as the whole column deforms.

The resulting theoretical curves are compared in Fig. 6 with the test results for two square columns of 76 mm (3 in) section at overall slenderness values of 32.7 and 92.5.

8. Conclusions

A series of tests on cold-formed square and rectangular hollow sections has been described including material tests, residual stress measurements, stub column and pin-ended column tests. The tests were performed for sections with fairly slender faces for which the transition from fully effective to partially effective occurred.

The yield strength of the material has been substantially enhanced by cold work, particularly in the corners. However a commensurate reduction in ductility of the material has occurred. The longitudinal residual stresses were found to be principally tensile on the outer surface and compressive on the inner surface with only a small net membrane stress in the section.

The limiting value of plate slenderness specified in the AISI Specification beyond which the flat element of a cold-formed square or rectangular hollow section would no longer be fully effective was accurately verified by the tests when the actual measured yield strengths were used. The AISI Class A column curve was found to be more representative of the concentrically loaded column tests than the Class B column curve.

Spatial plastic mechanisms, which included the rounded corners, were proposed for both the stub columns and long column tests. These mechanisms accurately simulated the unloading behaviour of the columns.

9. References

1. American Iron and Steel Institute, Specification for the Design of Cold-Formed Steel Structural Members, Washington DC, 1980

2. Australian Standards Association, Steel Structures Code (AS1250), Sydney, Australia, 1981

3. Bjorhovde, R., Strength and Behaviour of Cold-Formed HSS Columns, Structural Engineering Report No. 65, Department of Civil Engineering, University of Alberta, December, 1977.

4. Davison, T.A. and Birkemoe, P., Column Behaviour of Cold-Formed Hollow Structural Steel Shapes, Canadian Journal of Civil Engineering, Vol. 10, No. 1, 1983.

5. Dhalla, A.K. and Winter, G., Suggested Steel Ductility Requirements, Journal of the Structural Division, ASCE, Vol. 100, No. ST2, February 1974.

6. Haaijer, G., Plate Buckling in the Strain Hardening Range, Journal of the Engineering Mechanics Division, ASCE, April, 1957.

7. Johnston, B.G., Guide to Stability Design for Metal Structures, 3rd Edition, Wiley-Interscience, New York, 1976.

8. Kato, B. and Nishiyama, I., "Inelastic Local Buckling of Cold Formed Circular Hollow Section and Square Hollow Section Members", Japan-US Seminar on Inelastic Instability of Steel Structures and Structural Elements, Tokyo, 1981.

9. Kato, B., Cold Formed Welded Steel Tubular Members, Axially Compressed Structures,Chapter 5, Ed. R. Narayanan, Applied Science Publishers, London and New York, 1982.

10. Key, P.W. and Hancock, G.J., An Experimental Investigation of the Column Behaviour of Cold Formed Square Hollow Sections, Research Report No. R493, School of Civil and Mining Engineering, University of Sydney, June, 1985.

11. Key, P.W. and Hancock, G.J., Plastic Collapse Mechanisms for Cold Formed Square Hollow Section Columns, Research Report No. R526, School of Civil and Mining Engineering, University of Sydney, April,1986.

12. Mahendran, M., Box Columns with Combined Axial Compression and Torsional Loading, Ph.D. Thesis, Monash University, 1984.

13. Moxham, K., Buckling Tests on Individual Welded Plates in Compression, Cambridge University Engineering Department Research Report, C-Struct/TR. 3, 1971.

14. Murray, N.W., Introduction to the Theory of Thin-Walled Structures, Oxford University Press, 1984.

15. Packer, G.A. and Davies, G., Ultimate Strength of Overlapped Joints in Rectangular Hollow Section Trusses, Proc. Institution of Civil Engineers, Part 2,No. 73, 1982.

16. Rotter, J.M., Multiple Column Curves by Modifying Factors, Journal of Structural Engineering, ASCE, Vol. 108, No. ST7, 1982.

17. Sherman, D.R., Tentative Criteria for Structural Applications of Steel Tubing and Pipe, American Iron and Steel Institute, Washington DC, 1976.

TABLE I

MATERIAL PROPERTIES

SPECIMEN D x B x t (mm)	FORMED MATERIAL Location	σ_y	σ_u	$\Delta L/L$	σ_u/σ_y
76 x 76 x 2.0 (Series 1)	Face	425	499	5.4%	1.17
	Corner	531	588	2.3%	1.11
76 x 76 x 2.0 (Series 2)	Face	370	449	9.0%	1.21
	Corner	476	522	2.8%	1.10
152 x 152 x 4.9	Face	416*	475*	5.4%	1.14
	Corner	498	573	2.8%	1.15
203 x 203 x 6.3	Face	395	494	8.7%	1.25
	Corner	520	604	4.2%	1.16
254 x 254 x 6.3	Face	405	479	8.4%	1.18
	Corner	487	555	3.3%	1.14
102 x 51 x 2.0	Face	422	494	9.6%	1.17
	Corner	551	598	2.3%	1.09
127 x 51 x 3.6	Face	388	456	8.3%	1.17
	Corner	451	516	3.4%	1.15
127 x 64 x 4.0	Face	418	479	7.3%	1.15
	Corner	485	545	3.5%	1.13
152 x 76 x 4.9	Face	372	437	9.2%	1.17
	Corner	459	508	2.7%	1.11
203 x 102 x 4.9	Face	371	429	21.3%	1.16
	Corner	481	491	0.9%	1.02
254 x 152 x 6.3	Face	397	458	15.9%	1.15
	Corner	476	535	4.3%	1.12

Notes: 1. * Centre face yield stress factored to take account of yield stress variation across face.

2. All stresses in MPa (1 ksi = 6.895 MPa)

TABLE II

STUB COLUMN RESULTS

Specimen D x B x t (mm)	Full Section Area (mm^2)	P_{Sult} (kN)	P_{Scoup} (kN)	$\frac{P_{Sult}}{P_{Scoup}}$	AISI $Q_f P_{yf}$ (kN)	Australian Standard AS1250 $Q_f P_{yf}$ (kN)
76 x 76 x 2.0 (Series 1)	583	243	252	0.96	229	211
76 x 76 x 2.0 (Series 2)	583	-	221	-	-	197
152 x 152 x 4.9	2810	1283	1146	1.12	1169	1169
203 x 203 x 6.3	4830	2010 2015	1970	1.02 1.02	1908	1908
254 x 254 x 6.3	6110	2420 2500	2515	0.96 0.99	2197	2037
102 x 51 x 2.0	583	228 234	253	0.90 0.92	193	185
127 x 51 x 3.6	1180	470 472	468	1.00 1.01	458	447
127 x 64 x 4.0	1410	608 603	603	1.01 1.00	589	589
152 x 76 x 4.9	2060	785 784	793	0.99 0.99	766	766
203 x 102 x 4.9	2810	1090 1095	1076	1.01 1.02	972	927
254 x 152 x 6.3	4830	1950	1957	1.00	1793	1715

1 in^2 = 645 mm^2
1 kip = 4.45 kN

TABLE III

PIN-ENDED COLUMN RESULTS

Section D x B x t (mm)	L/r	P_{max} (kN)	
		Concentric	Eccentric
76 x 76 x 2.0	15.3	222	226
(Series 1)	32.7	220	210
	62.7	200	190
	92.5	144	108
76 x 76 x 2.0	25.9	-	204
(Series 2)	47.8	-	200
	79.2	-	132
	92.5	-	104
152 x 152 x 4.9	20.3	1250	1212
	37.7	1167	1108
	67.8	898	824
	98.0	560	486
203 x 203 x 6.3	35.7	1823	1807
	65.7	1477	1280
	95.7	846	784

1 kip = 4.45 kN

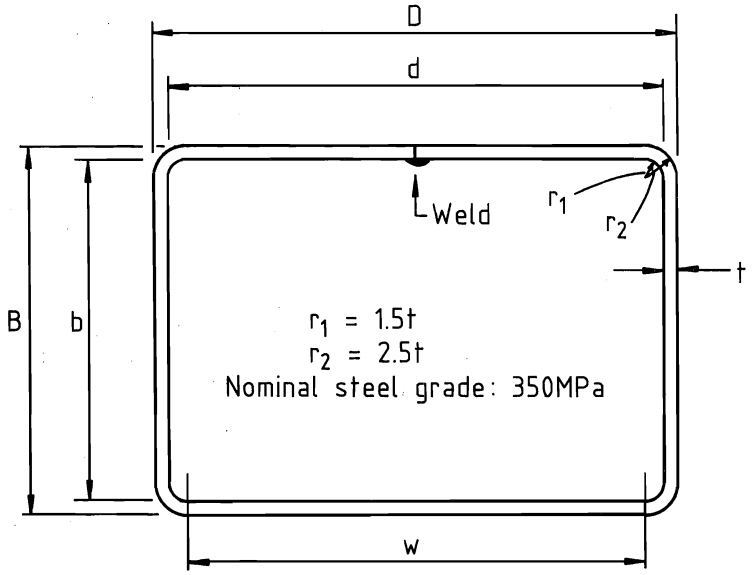

(a) Section Dimension Nomenclature

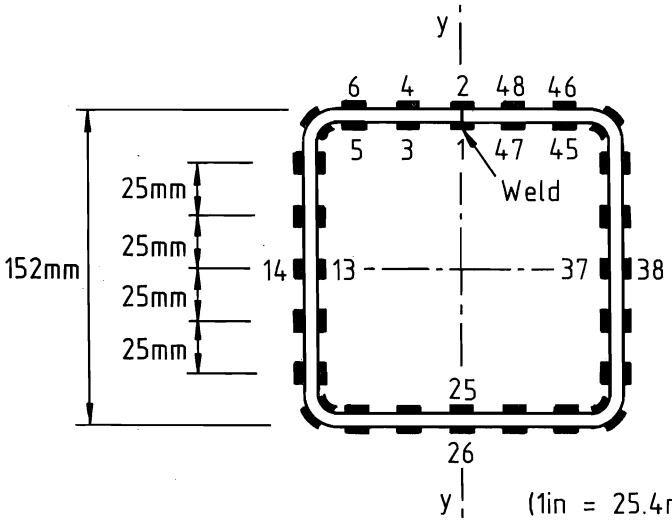

(b) Strain Gauge Layout for Residual Stress Measurement

FIG.1 SECTION GEOMETRY

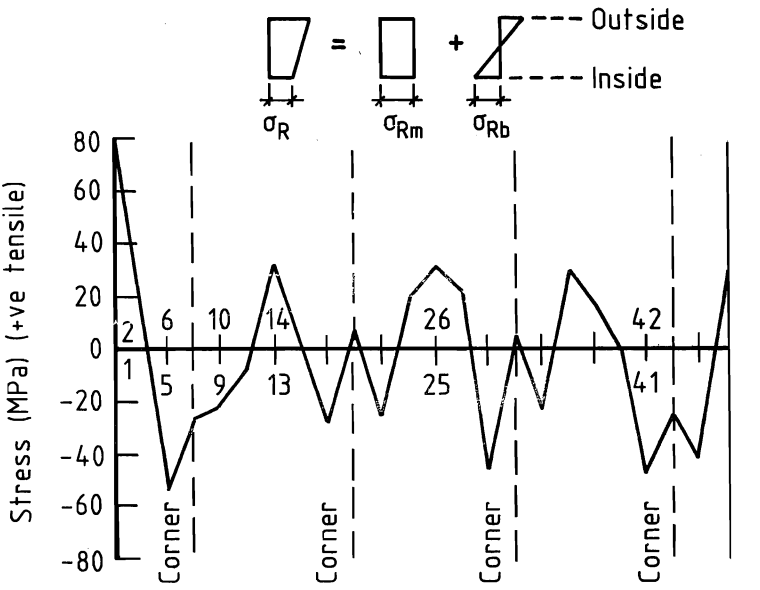

(a) Longitudinal Membrane Stress (σ_{Rm})

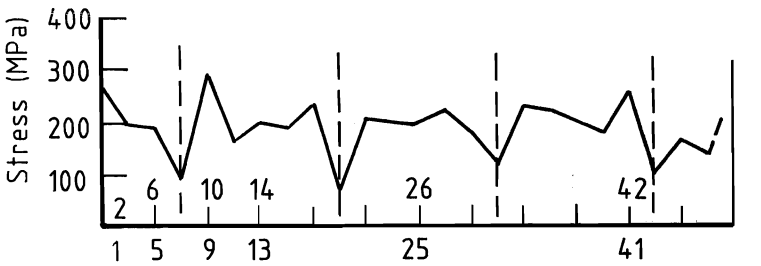

(b) Longitudinal Bending Stress (σ_{Rb})

FIG.2 MEASURED RESIDUAL STRESSES

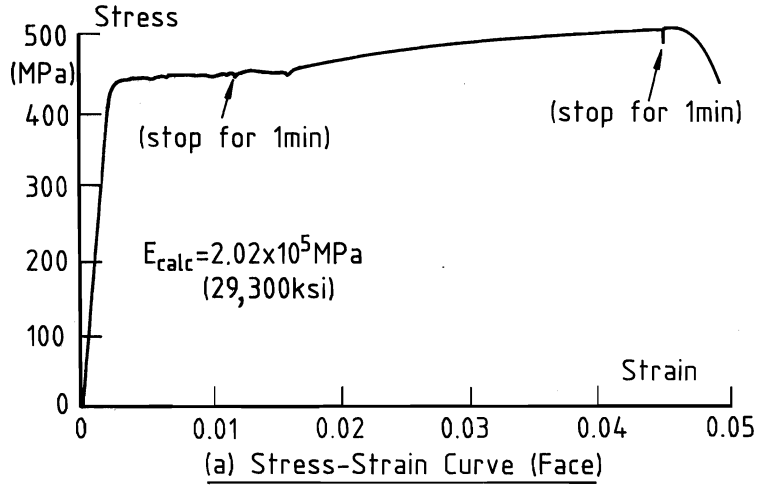

(a) Stress-Strain Curve (Face)

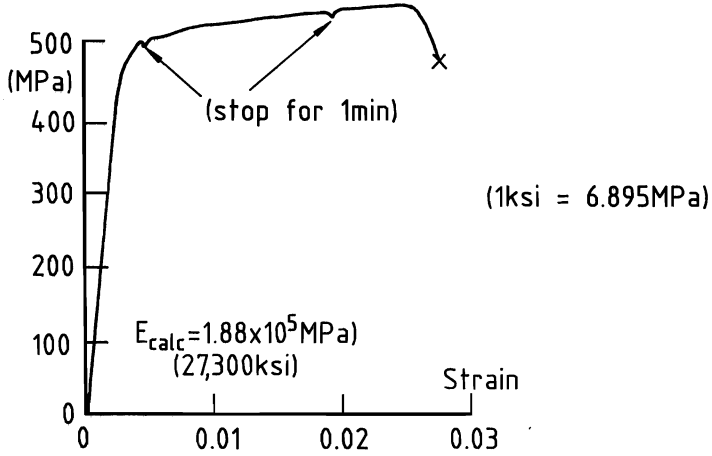

(b) Stress-Strain Curve (Corner)

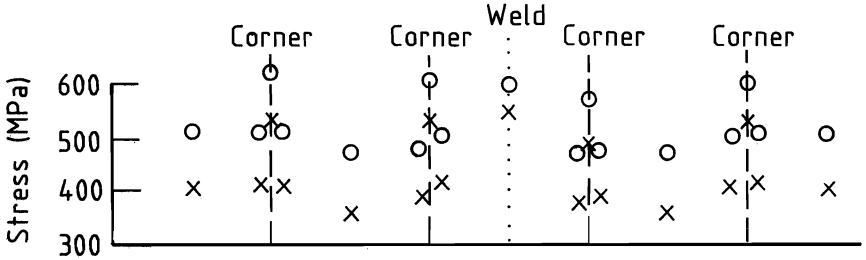

(c) Distribution of Yield Stress (x) and Ultimate Tensile Strength (o)

FIG.3 MATERIAL PROPERTIES

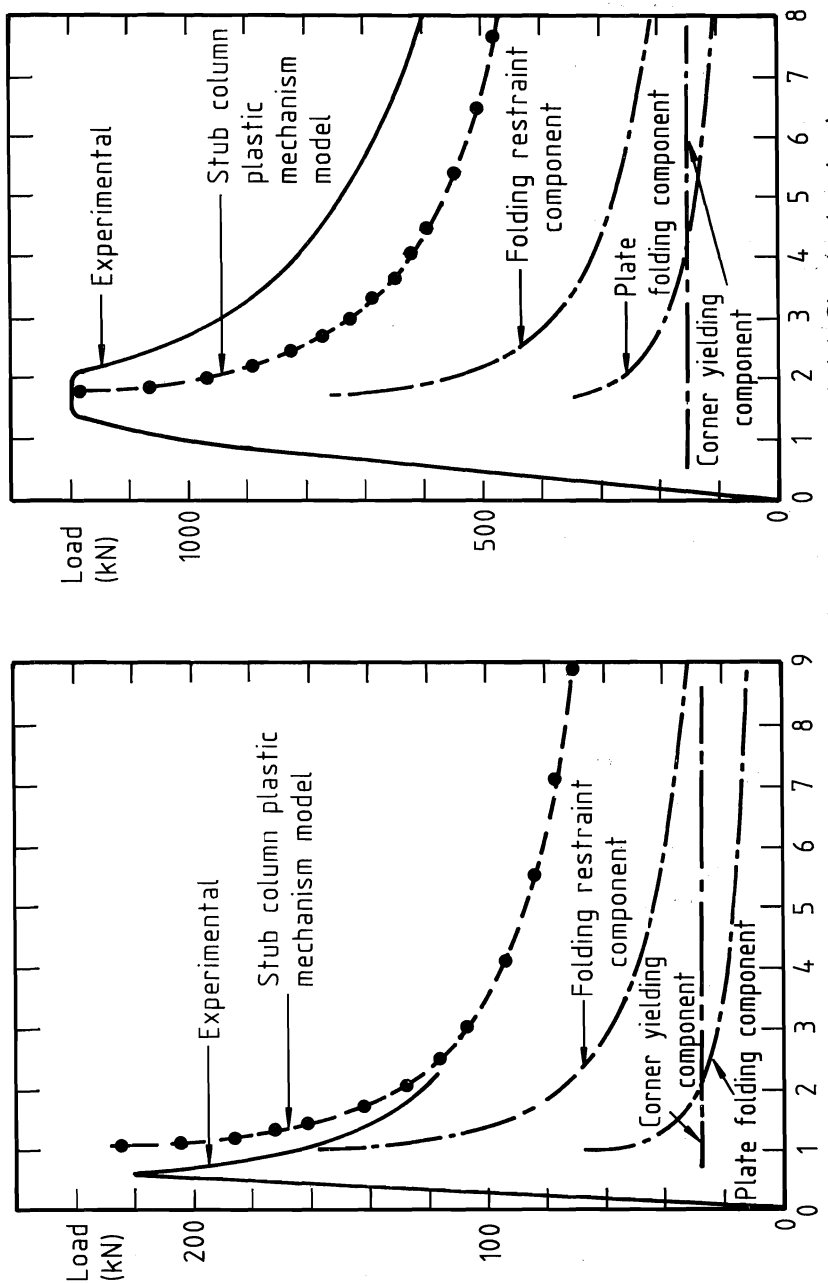

FIG.4 STUB COLUMN LOAD-SHORTENING CURVES

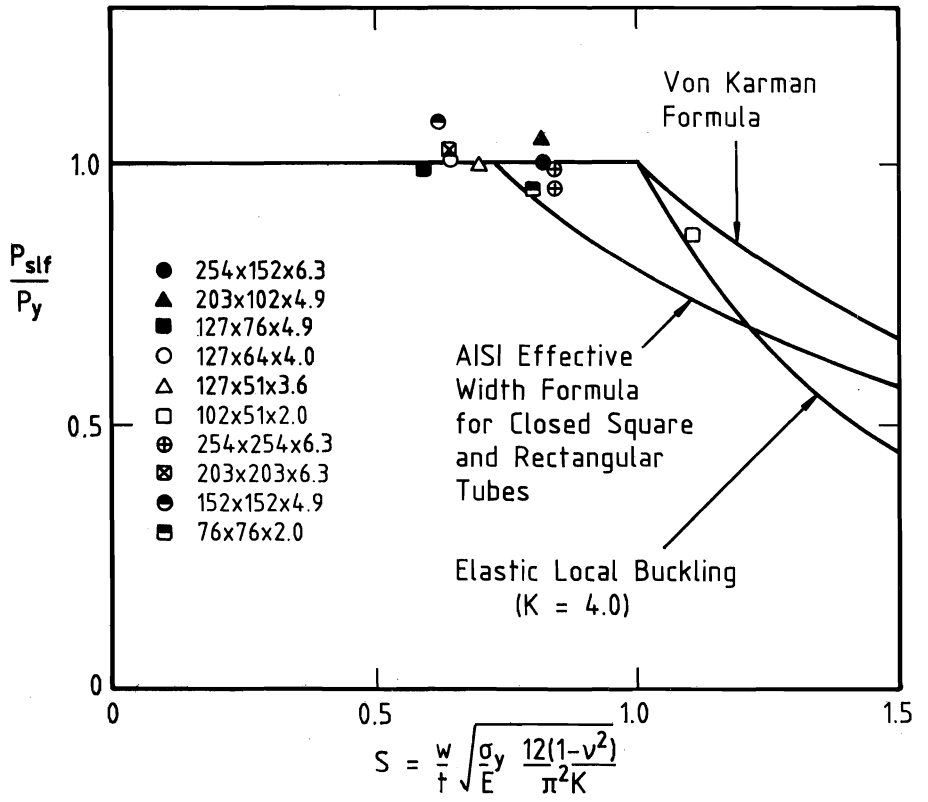

FIG.5 PLATE STRENGTH VERSUS SLENDERNESS

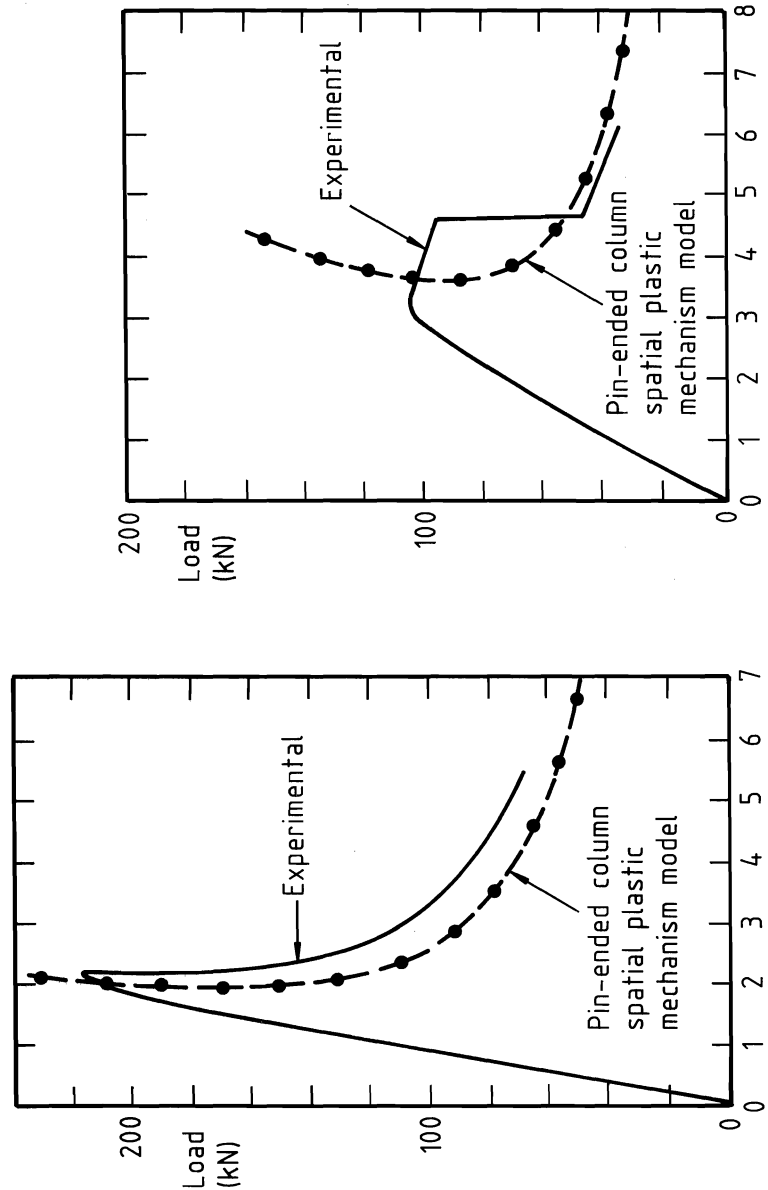

FIG.6 PIN-ENDED COLUMN LOAD AXIAL SHORTENING CURVES

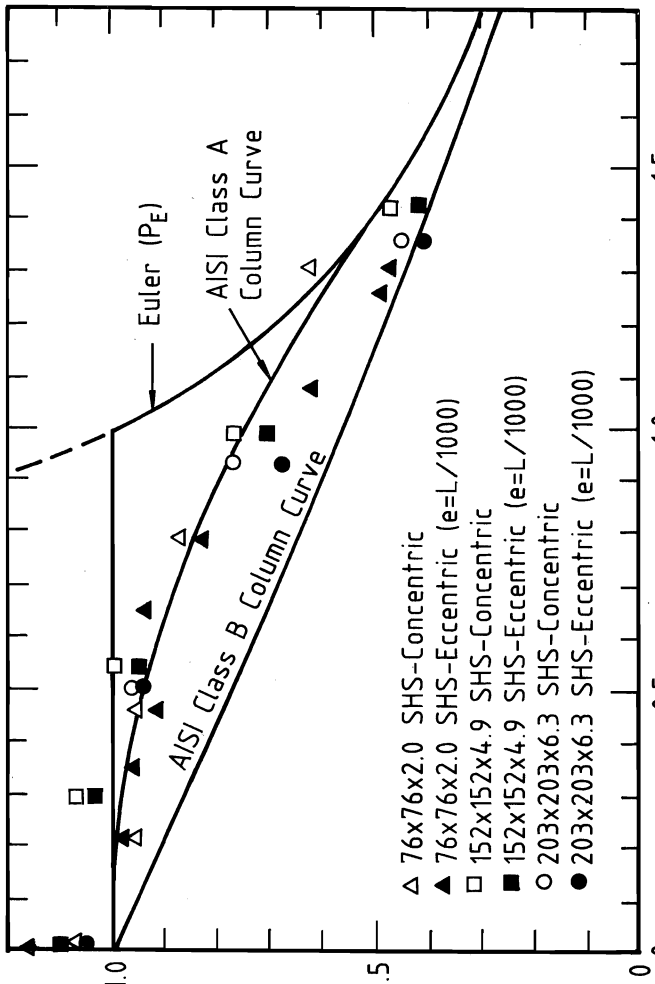

FIG.7 COMPARISON OF AISI COLUMN CURVES WITH TEST RESULTS

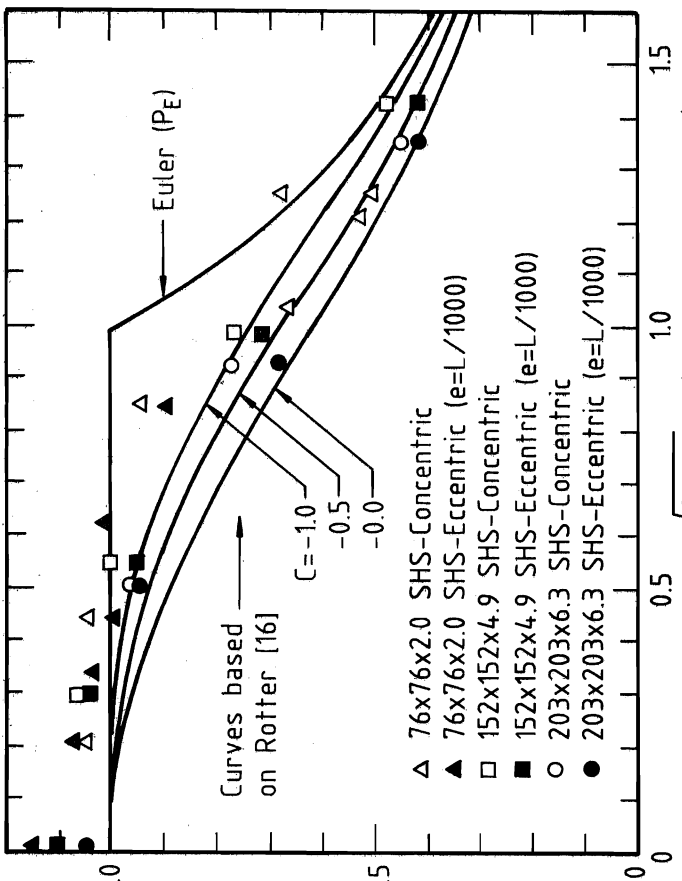

FIG.8 COMPARISON OF AUSTRALIAN LIMIT STATE STEEL STRUCTURES CODE COLUMN CURVES WITH TEST RESULTS

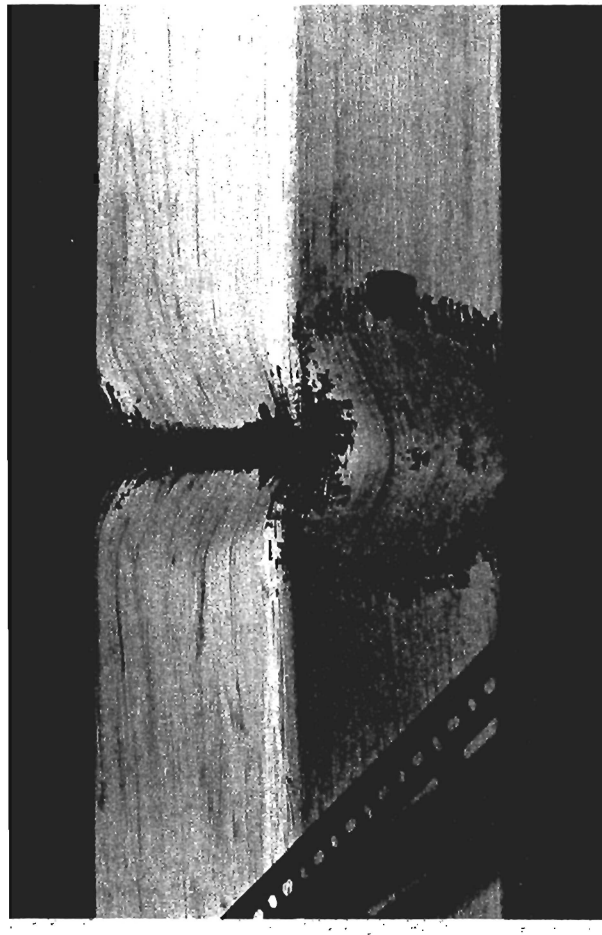

FIG.9 STUB COLUMN LOCAL BUCKLING FAILURE MODE

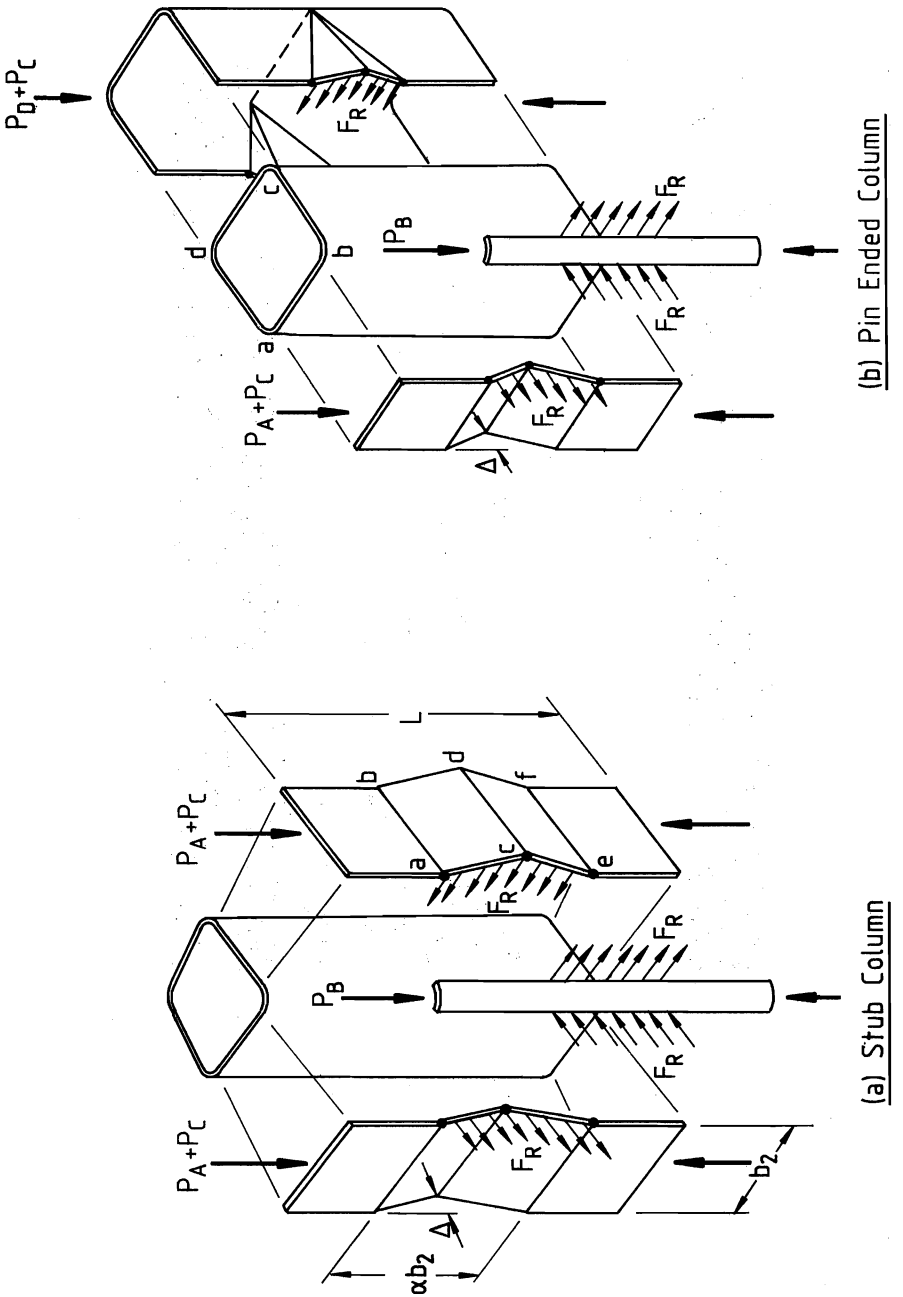

FIG.10 SPATIAL PLASTIC MECHANISMS

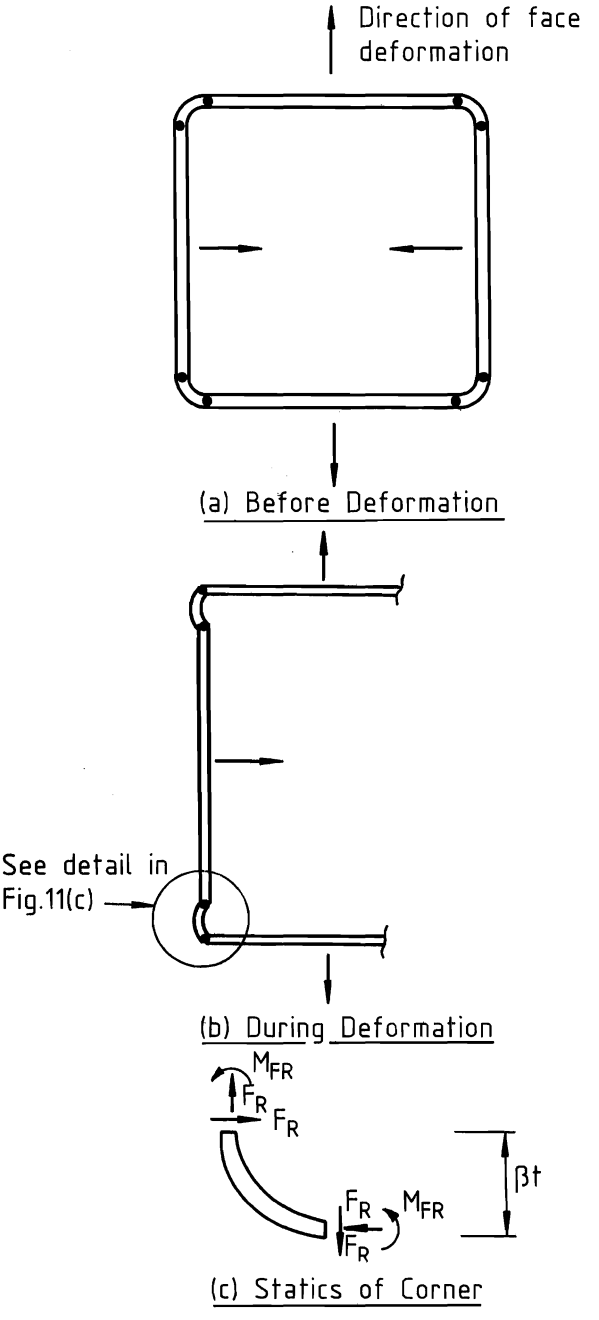

FIG.11 CORNER FOLDING RESTRAINT MODEL